RSC Advances

REVIEW

View Article Online
View Journal | View Issue

Cite this: *RSC Adv.*, 2024, **14**, 30566

Recent advances in noble metal-based catalysts for CO oxidation

Sheng Wang,[a] Xiaoman Li,[b] Chengyue Lai,[c] Yaping Zhang,[b] Xiao Lin[b] and Shipeng Ding *[b]

Carbon monoxide, one of the major pollutants in the air, is mainly produced due to the incomplete combustion of fossil fuels such as coal and oil. Among all the techniques developed for removing CO, catalytic oxidation has been considered one of the most effective approaches, and the commonly used catalysts include metal oxides and noble metals. Noble metal attracted extensive attention due to its good catalytic performance at low temperatures and high resistance to poisoning. The review summarizes the recent advances of noble metals including Pt, Pd, Au, Ru, Rh, and Ir in CO oxidation. The effect of support, metal doping, the particle size of noble metals, and the hydroxyl groups on CO oxidation is discussed. Besides, the metal-support interaction on the stability and activity is also involved in this review. Finally, the challenges and opportunities of supported noble metal catalysts in practical CO oxidation are proposed.

Received 15th July 2024
Accepted 20th September 2024

DOI: 10.1039/d4ra05102e

rsc.li/rsc-advances

1 Introduction

Industrial exhaust and automobile exhaust have become the primary sources of atmospheric pollution, and CO is one of the most abundant components in exhaust gas.[1–6] CO is mainly produced from the incomplete combustion of fuel in oxygen-deficient conditions. It was reported that 90% of the CO emission in urban areas is from motor vehicles. CO is also derived to numerous environmental and health issues. For example, when the CO concentration in the environment reaches 0.1% above, humans may be poisoned and die within minutes. Therefore, it is essential to find an effective method to purify CO. Among all the techniques, catalytic oxidation is one of the simple, inexpensive, and effective methods to remove CO. Besides, CO oxidation was considered an important probe reaction to investigate the structure and metal-support interaction of the supported catalysts. In the past few decades, transition metal oxides and noble metal catalysts have been developed for the catalytic purification of CO. Among them, noble metal catalysts received much attention due to their excellent low-temperature CO oxidation activity.[7–11] For example, it was reported that the supported Au nanoparticles could oxidize CO even at −70 °C, though the bulk Au is generally inert.[12] Pt and Pd have been extensively applied as the main components of three-way catalysts to purify CO in diesel vehicle exhaust. Apart from the purification of CO emitted from the industrial exhaust and automobile exhaust, the selective removal of trace amount of CO in H_2-rich conditions is vital for H_2 fuel cell, as the H_2 produced from methane streaming and water gas shift reaction usually contains a low concentration of CO, which deactivated the Pt electrode in the proton-exchange membrane fuel cells. In this scenario, the key was to fully remove CO without H_2 oxidation. Various catalyst including both noble and non-noble catalysts have been developed for preferential CO oxidation. It was recently reported that single-atom catalysts showed decent preferential CO activity, which might be due to the relatively weak H_2 activation ability. On the other hand, the stability of the single-atom catalysts remains challenging. The coordination unsaturated single-atom noble metal species tend to aggregate into nanoparticles under reductive conditions. A knowledge gas on how to develop a catalyst with high stability, activity and selectivity for CO preferential CO still existed. The noble metal species were generally supported on metal oxides in those catalysts. Apart from the intrinsic properties of noble metal, the characteristics of the metal oxides also significantly affected the CO catalytic oxidation performance.

This paper reviewed the recent progress of supported noble metal catalysts (including Pt, Pd, Au, Ru, Rh, and Ir.) in CO catalytic oxidation. Although some reviews have summarized the progress of supported catalysts in CO oxidation, a comprehensive review of the recent advances (particularly past three years) of noble metal-based catalysts in CO oxidation is still limited Table 1. This review critically reviewed the characteristics of different supported noble metal catalysts and the key factors affecting CO catalytic oxidation are discussed, including catalyst carrier, dopant, metal particle size, hydroxyl group, *etc.*

[a]*National Energy Group Science and Technology Research Institute, Nanjing, 210031, Jiangsu, China*

[b]*Key Laboratory of Energy Thermal Conversion and Control of Ministry of Education, School of Energy and Environment, Southeast University, Nanjing, 210096, Jiangsu, China. E-mail: dingshp@seu.edu.cn*

[c]*Chengdu Academy of Environmental Sciences, Chengdu, 610072, China*

Table 1 The CO oxidation performance of parts of noble metal-based catalysts reported in the literature

	Reaction conditions						
Catalysts	Temperature (°C)	WHSV (mL g^{-1} h^{-1})	CO (ppm)	O_2 (%)	CO conversion (%)	Temperature (°C)	Ref.
0.5%Pt_n/ND@G	30–200	12 000	10 000	1	100	120	13
Pt/TiO_2	60–160	47 900	8000	16	100	100	14
4.5%Pt/CeO_2	50–500	60 000	1000	10	50	85	15
CoO_x/Pt/CeO_2	−50–85	75 000	10 000	20	100	20	16
Pt-CD/Al_2O_3	−80–80	18 000	10 000	1	100	−20	7
1%Pt-2%Bi/SiO_2	20–160	134 000	10 000	20	100	100	17
1%Pt/SiO_2	20–160	134 000	10 000	20	100	150	17
0.1%Pt/Sb–SnO_2	100–450	120 000	10 000	1	100	240	18
0.1%Pt/SnO_2	100–450	120 000	10 000	1	100	270	18
0.1%Pt/SiO_2	100–450	120 000	10 000	1	100	270	18
Pt/CeO_2	50–250	80 000	6000	0.6	100	180	19
Pt/Nb_2O_5	50–250	80 000	6000	0.6	14.9	180	19
Pd/CeO_2(111)	50–300	60 000	20 000	2	100	150	20
Pd/CeO_2(100)	50–300	60 000	20 000	2	100	200	20
Pd/CeO_2–SnO_2-800	−10–450	240 000[a]	2000	1	50	45	21
Pd/CeO_2-800	−10–450	240 000[a]	2000	1	50	60	21
Pd/$Ce_{0.3}Zr_{0.7}O_2$	100–300	600 000	10 000	0.5	50	134	10
Pd/$Ce_{0.7}Zr_{0.3}O_2$	100–300	600 000	10 000	0.5	50	163	10
Pd_1@HEFO	50–300	40 000	10 000	20	100	170	22
Pd@CeO_2	50–300	40 000	10 000	20	100	253	22
Pd/α-Fe_2O_3	−50–250	15 000	10 000	20	100	120	23
Pd/γ-Fe_2O_3	−50–250	15 000	10 000	20	100	80	23
Pd/MnO_x–CeO_2	50–450	40 000[a]	20 000	5	100	50	24
$Co_{0.24}Pd_{0.76}$	25–200	60 000	10 000	4	100	110	25
Au_3Pd_7/TiO_2	50–250	48 000[a]	1000	10	50	139	26
PdFe/CeO_2-HT	25–160	120 000	10 000	1	100	125	27
Pd-SBA-15	40–180	30 000	40 000	20	100	115	28
Au–Rh/NT	0–300	150 000	10 000	1	100	68	29
Au/NT	0–300	150 000	10 000	1	100	179	29
CeOx@Au/SiO_2	50–450	16 000	20 000	16	100	180	30
Au/SiO_2	50–450	16 000	20 000	16	100	340	30
Au/La(6.6)/HAP	40–120	60 000	10 000	1	100	60	31
Au/HAP	40–120	60 000	10 000	1	80	60	31
Au/CuO	0–250	15 000	10 000	21	100	55	32
Au/Cu_2O	0–250	15 000	10 000	21	100	200	32
Ru–ZrO_2	80–200	12 000[a]	10 000	0.5	95	100	11
Ru–TiO_2	80–200	12 000[a]	10 000	0.5	90	100	11
5Ru/CeO_2(110)	25–425	36 000	10 000	20	10	71	33
5Ru/CeO_2(111)	25–425	36 000	10 000	20	10	99	33
5Ru/CeO_2 (100)	25–425	36 000	10 000	20	10	96	33
$Cu_{0.2}Ru_{0.8}$/γ-Al_2O_3	80–160	20 000	10 000	1	50	109	34
Ru/γ-Al_2O_3	80–160	20 000	10 000	1	50	155	34
Rh/Ce-MCM-41	100–350	75 000	10 000	1	100	167	35
Rh/MCM-41	100–350	75 000	10 000	1	78	270	35
Rh_1/ZnO-nw	150–400	40 000	10 000	1	100	210	8
3%Ir/BFA	0–220	20 000	10 000	1	100	20	9
2Fe/Ir/SiO_2-350	20–220	18 000	10 000	1	100	80	36

[a] Gaseous hourly space velocity (h^{-1}).

This review aims to provide an overview of the practical application of noble metal catalysts in CO catalytic purification Fig. 1.

The conventional methods to prepare noble-metal based catalysts including coprecipitation, impregnation, hydrothermal and *et al.* For example, it was reported that atomically dispersed Pt_1/FeO_x was fabricated by co-precipitation *via* finely controlling the Pt loading, pH value and temperature for CO oxidation.[37] Similarly, Au single-atom and nanoparticle species, isolated Ir species dispersed on FeO_x were also fabricated *via* the coprecipitation for CO oxidation,[38] in which CO and O_2 molecules reacted in the interface of sites through a Langmuir–Hinshelwood mechanism. Apart from coprecipitation, other approaches were also applied. *Via* optimizing the solution pH during the synthesis procedure, atomically dispersed Pt species was anchored on TiO_2 and displayed higher CO oxidation

performance than the nanoparticle counterparts.[39] Zhang and co-workers anchored isolated Pt atoms within the pore structure of Al_2O_3 *via* a Pluronic P-123 assisted sol–gel approach for CO oxidation.[40] Other unconventional methods such photochemical reduction, flame spray pyrolysis, and electrochemical deposition were also reported for CO oxidation.[41–43] The methods to prepare noble-metal based catalysts for CO oxidation is not the focus of the manuscript. The following section will be discussed based on the type of noble metals.

2 Pt-based catalyst

Pt-based catalysts were extensively studied in CO oxidation and have been considered as one of the most active noble metals for CO catalytic oxidation.[44–50] The following section will summarize the recent progress of Pt-based catalysts in CO oxidation. Particular effort was given to the structure–performance relationship investigation, including the effect of Pt particle size, metal doping, the role of the hydroxyl group, and the support effect.[51–61]

2.1 Effect of metal particle size

The particle size of Pt significantly affected the activity of CO catalytic oxidation. It is still controversial which one was more active in CO oxidation among Pt single-atom, nanoclusters, and nanoparticles. Beniya *et al.* investigated the relationship between CO oxidation activity and the size of Pt species and successfully established the relationship of CO oxidation activity as a function of Pt sizes on TiO_2.[62] The ratio of metal to cationic Pt atoms is linearly correlated to the CO oxidation activity. Jia *et al.* loaded Pt single atoms (Pt_1), clusters (Pt_n), and nanoparticles (Pt_p) onto nanodiamond/graphene (ND@G) composite carriers and explored the structure of the active sites of the catalysts for the oxidation of CO.[63] Due to the weak CO adsorption, strong O_2 dissociative adsorption of Pt clusters, and the near 100% Pt dispersion, the fully exposed Pt cluster (0.5 wt%) loaded on ND@G possessed optimal low-temperature CO oxidation activity (Fig. 2a). Dessal *et al.* investigated the structural stability of Pt/γ-Al_2O_3 single-atom catalysts for CO oxidation and their catalytic properties.[64] It was indicated that isolated Pt ions gradually aggregated to form partially oxidized Pt clusters during the reaction. Since clusters had better activity than isolated atoms, the formation of Pt clusters during the reaction process or after hydrogen treatment increased the CO oxidation activity of Pt species. Cai *et al.* showed that the Pt species on Pt/TiO_2 catalyst had higher dispersion and smaller Pt particle size after calcination pretreatment of TiO_2 at 700 °C.[14] The reduced adsorption capacity of the catalyst for CO and CO_2 allowed the complete conversion of CO at 100 °C, which was 40 °C lower than that of the samples without calcination pretreatment. The concentration of noble metal on the catalyst surface also significantly affected the CO oxidation activity. By increasing Pt loading, Maurer *et al.* increased the surface noble metal concentration (SNMC) of the Pt/CeO_2 catalyst by four times, thereby reducing the distance between Pt species. The high surface noble metal concentration promoted the formation of active Pt clusters at low temperatures. It increased the reaction rate of CO oxidation, which further proved that the surface noble metal concentration was the key to affecting the low-temperature activity of the Pt/CeO_2 catalyst (Fig. 2b).[15] Chen and co-workers demonstrated that CO-rich conditions induced the reconstruction of Pt species from $Pt_1(CO)$ to $Pt_8(CO)_9$ complex using first-principles investigation.[45] Besides, a linear scaling relationship was established between CO_2 formation rate and O adsorption energy among single atoms, clusters, and nanocatalysts (Fig. 2c).

2.2 Elemental doping

Elemental doping is a conventional method to improve the CO catalytic activity of Pt-based catalysts.[65] Wang *et al.* doped BaO as an additive into Pt/La–Al_2O_3 catalyst to effectively stabilized the PtO_x catalytic sites on the La–Al_2O_3 surface.[66] The catalyst still had almost 100% atomic dispersion after hydrothermal aging at 650 °C, indicating the good stability and sintering resistance of the catalyst. Lee *et al.* investigated the effect of MnO_x doping on the CO oxidation activity of Pt/Al_2O_3 catalysts by atomic layer deposition (ALD).[67] Compared with the unmodified Pt/Al_2O_3 catalyst, the addition of MnO_x improved the durability of the catalysts and inhibited the agglomeration of Pt particles after thermal aging at 1073 K. The modified catalysts generated highly active Pt–MnO_x interfacial sites to increase the CO oxidation rate. Song *et al.* introduced transition metal oxides (MO_x, M = Fe, Co, and Ni) into Pt/CeO_2 catalysts and investigated the role of transition metal oxides in CO oxidation.[16] The variable chemical valence states of Fe and Co-promoted the electron transfer from Pt to MO_x, enhancing the carrier's redox properties and the ability to activate oxygen molecules. The stability of the catalysts mainly depended on the ability of the carriers to provide oxygen. CoO_x–Pt/CeO_2 and NiO_x–Pt/CeO_2 were highly stable under high humidity conditions due to their ability to reversibly restore the reactive oxygen species consumed by the reaction. CoO_x was the optimal choice for improving the CO oxidation performance of Pt/CeO_2 catalysts because it could simultaneously enhance the activity and stability of Pt/CeO_2. Nan *et al.* modified the Pt-based catalyst by adding BiO_x.[17] The strong interaction between BiO_x and Pt resulted in $Pt_xBi_yO_z$ clusters with excellent sintering resistance in the CO oxidation reaction. The addition of BiO_x resulted in the formation of a unique Pt–$[O]_x$–Bi cluster structure on the surface of the catalysts, which allowed the efficient activation and dissociation of oxygen molecules at low temperatures. At the same time, this structure prevented poisoning of Pt species due to CO supersaturation adsorption and efficiently activated CO molecules, thereby reducing the activation energy of CO oxidation. Liebertseder designed a TiO_2–CeO_x–Pt hollow catalyst by a liquid-phase strategy using NaCl as a template (Fig. 2d).[44] The prepared catalyst showed stable performance in the low-temperature CO oxidation.

2.3 Effects of hydroxyl groups

Hydroxyl species played a crucial role in improving the catalytic oxidation of CO over Pt-based catalysts. Chen *et al.* synthesized

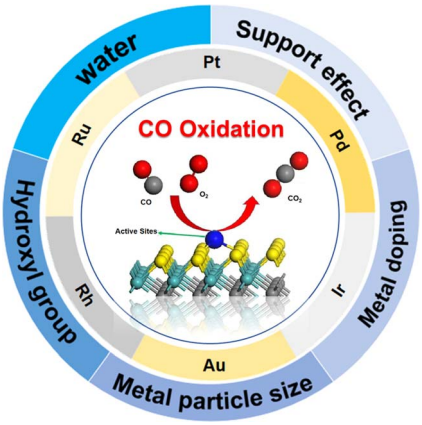

Fig. 1 The overview of the noble-based catalysts in CO oxidation.

the Pt/Al_2O_3 catalyst by a refined colloidal deposition method with 100% CO conversion at low temperatures.[10] Structural characterization combined with theoretical calculations demonstrated that CO adsorbed on the kink sites of $Pt(OH)_x$ could react with OH on the platform sites to form CO_2, whereas O_2 molecules were activated on the terrace sites of $Pt(OH)_x$ to regenerate OH groups. The kink and terrace sites of Pt species synergy suppressed the competitive adsorption between CO and O_2, thus decreasing the reaction energy barrier for CO oxidation. Similarly, they also tested the activity of the Pt/Al_2O_3 in CO catalytic oxidation under hydrogen-rich conditions.[68] The Pt/Al_2O_3 catalyst possessed the active sites with both $Pt(OH)_x$ and metallic Pt, weakening the competitive adsorption between CO and H_2 and facilitating O_2 activation. The catalyst exhibited 100% CO conversion and 100% CO_2 selectivity in the temperature range of −30 to 120 °C. Chai *et al.* reported that water molecules on Pt(111) affected the low-temperature oxidation of CO under near-ambient conditions.[1] The results showed that H_2O was activated on Pt(111) to generate the key intermediates (the reversibly adsorbed OH groups and the irreversibly adsorbed COOH groups), which significantly increased the CO oxidation in the temperature range of 290–320 K. Liu *et al.* investigated the surface chemistry of ZnO/Pt(111) catalysts for CO oxidation.[69] The reaction rate of ZnO/Pt(111) was 30% higher than that of Pt(111) in the range from room temperature to 410 K. Meanwhile, the carboxyl groups formed at low temperature, and the OH species located at the Pt/ZnO acted as the intermediates and co-catalysts respectively to promote the CO oxidation due to the synergistic interaction between ZnO and Pt. Apart from experimental investigation, theoretical calculations were also applied to study the effect of OH groups on CO oxidation.[60] Fig. 2e showed that the d-band center of Co is shifted from −4.14 to −3.99 eV in the presence of the OH group, indicating the activity enhancement of Co species by OH modification.

2.4 Support effect

The catalytic activity of Pt-based catalysts in CO oxidation is also related to the support. Bae *et al.* compared the catalytic performance of $Pt/Sb–SnO_2$, Pt/SnO_2, and Pt/SiO_2 catalysts with the same Pt loading in CO oxidation.[18] It was discovered that $Pt/Sb–SnO_2$ showed the best catalytic activity and high durability. Further studies demonstrated that $Pt/Sb–SnO_2$ had the most abundant surface oxygen and was hard to form surface carbonates during the reaction process, thus promoting the CO oxidation reaction. Cai *et al.* prepared Pt/CoO_x by dispersing Pt on CoO_x nanoclusters *via* the selective atomic layer deposition method. The highly dispersed Pt maximized the interface and enhanced the CO-PROX activity of Pt/CoO_x, resulting in almost 100% CO conversion and CO_2 selectivity at room temperature of Pt/CoO_x.[70] Compared with conventional Pt/Co_3O_4, Pt/CoO_x exhibited weaker adsorption of CO and lower O_2 activation energy barriers, which indicated that different preparation methods could significantly affect the state of the active sites on the support, thus in turn affecting the catalytic performance. Wang *et al.* compared the CO oxidation performance of Pt/CeO_2 and Pt/Nb_2O_5 catalysts.[19] The Pt/CeO_2 catalysts showed higher activity than the Pt/Nb_2O_5 catalysts for CO oxidation due to the easier activation of oxygen on CeO_2, which has abundant oxygen vacancies.

3 Pd-based catalysts

Apart from Pt, Pd-based catalysts were also extensively studied in CO oxidation.[71–74] The influence of the support, bimetallic doping, and Pd particle size will be summarized in the following section.

3.1 Support effect

The support also markedly affected the catalytic performance of Pd-based catalysts. Spezzati *et al.* demonstrated that the different catalytic activity in CO oxidation of $Pd/CeO_2(111)$ and $Pd/CeO_2(100)$ was mainly attributed to the difference in free energy barriers.[20] Slavinskaya *et al.* prepared Pd/CeO_2, Pd/SnO_2, and $Pd/CeO_2–SnO_2$ catalysts and compared their catalytic activity in CO oxidation.[21] The results indicated that $Pd/CeO_2–SnO_2$ had more active lattice oxygen and more thermally stable PdO_x(s)/Pd–O–Ce(s) clusters, which resulted in relatively better low-temperature CO oxidation activity and excellent thermal stability. Li *et al.* investigated the effect of Pd-support interactions on CO oxidation performance for Pd/CeO_2 and $Pd/CeO_2–ZrO_2$ catalysts.[10] As shown in Fig. 3a, the interactions between Pd and the support were attributed to the surface reactive oxygen species of the support. Pd existed in an ionic state on Pd/CeO_2 but in a metallic state on $Pd/Ce_{0.3}Zr_{0.7}O_2$. Although the dispersion of Pd was higher in the Pd/CeO_2, the weaker adsorption of CO by Pd in the ionic state resulted in lower TOFs. In addition, further studies demonstrated that the pretreatment conditions could dramatically change the Pd-support interactions. The hydrothermal-aged Pd/CeO_2 showed weak $Pd–CeO_2$ interactions and poor catalytic performance, while the hydrothermal-aged $Pd/Ce_{0.7}Zr_{0.3}O_2$ exhibited higher Pd dispersion and excellent activity. Xu *et al.* synthesized a sinter-resistant Pd single-atom catalyst Pd_1@HEFO by a combination of mechanical milling and high-temperature calcination

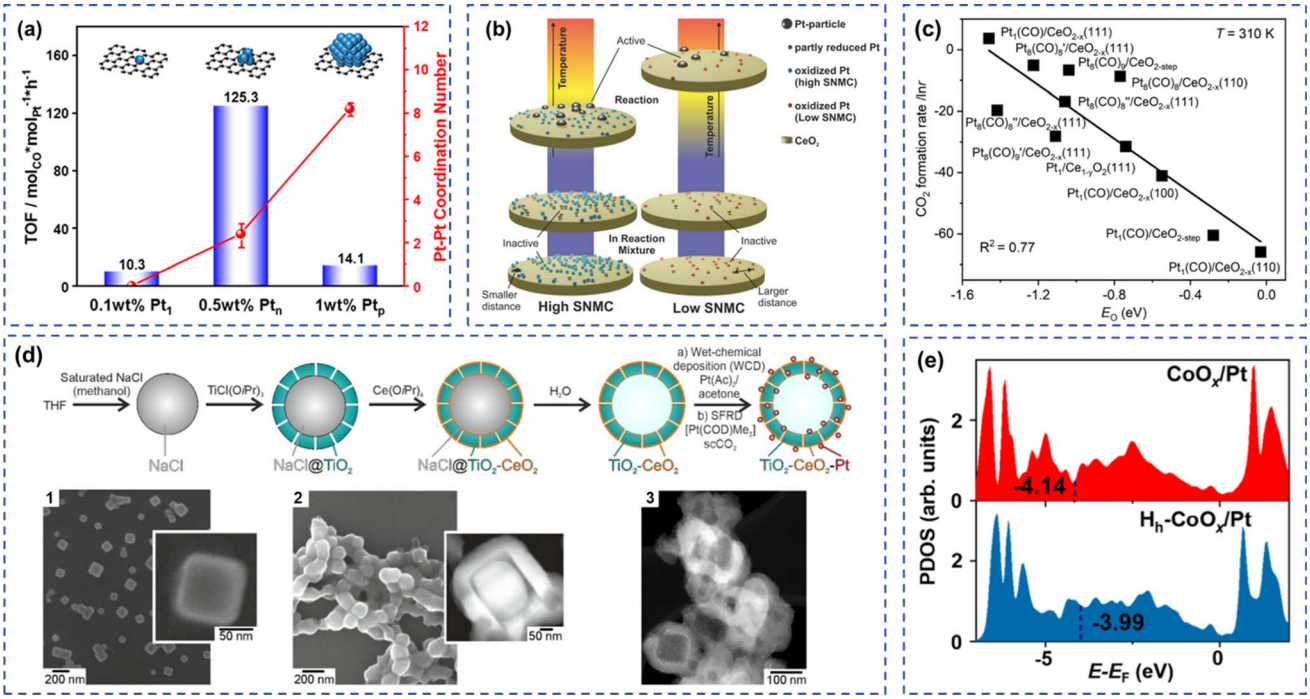

Fig. 2 (a) Relationship between the Pt–Pt shell coordination numbers and their TOF over Pt single, nanocluster, and nanoparticle. Reproduced with permission from ref. 63 Copyright 2022, American Chemical Society. (b) The scheme of cluster formation model under reaction conditions and the dependence of CO oxidation activity on the surface noble metal concentration (SNMC). Reproduced with permission from ref. 15 Copyright 2022, American Chemical Society. (c) Copyright 2024, American Chemical Society. (d)The synthesis of TiO_2–CeO_x–Pt hollow catalyst by a liquid-phase strategy Reproduced with permission from ref. 44 Copyright 2024, Wiley-VCH GmbH. (e) The projected density of states of Co species in CoOx/Pt(111) and H_hCoO_x/Pt(111).[60] Copyright 2024, American Chemical Society.

method.[22] The results of characterizations indicated that the Pd atoms were doped into the crystal lattice of HEFO through the formation of stable Pd–O–M (M = Ce/Zr/La) bonds. Compared with conventional Pd@CeO_2 catalysts, Pd_1@HEFO showed higher reducibility of lattice oxygen and had more stable Pd–O–M species, resulting in superior CO oxidation activity and better thermal stability. Wang *et al.* prepared Pd/Fe_2O_3 catalysts with different Fe_2O_3 crystal types by deposition precipitation method and found that Pd/γ-Fe_2O_3 showed better catalytic performance than Pd/α-Fe_2O_3 in CO oxidation.[23] Further characterization showed that the strong interaction between Pd and γ-Fe_2O_3 increased the concentration of Fe^{2+}, promoted the redox cycle between Fe^{3+} and Fe^{2+}, and facilitated the activation of oxygen molecules, thus exhibiting higher catalytic activity for CO oxidation. In contrast, when Pd was loaded on α-Fe_2O_3, the carbonate and bicarbonate species were easily formed on the catalyst surface, which inhibited the oxygen activation process, resulting in lower catalytic activity. Wang *et al.* investigated the low-temperature CO oxidation activity of Pd-doped MnO_x–CeO_2 (MC) solid solution catalysts.[24] In the process of calcination, highly dispersed PdO that exhibited catalytic activity toward CO oxidation was formed on CeO_2 and MC supports. However, Pd^{2+} on CeO_2 would be reduced to Pd^0 during CO oxidation, whereas MC can promote the transfer of lattice oxygen and thus stabilize Pd^{2+}. In addition, CO/O_2 transient pulse experiments confirmed that MC showed higher reducibility than CeO_2 and could facilitate CO oxidation at 50 °C.

3.2 Bimetallic catalysts

Pd-based bimetallic catalysts are also widely used in CO oxidation reactions.[76] Wu *et al.* investigated the surface evolution of CoPd alloy nanoparticles under CO oxidation reaction and revealed the correlation between its catalytic activity and surface composition.[25] The synergistic effect between Pd and CoO_x promoted the CO oxidation activity of the bimetallic catalysts, as Co was biased to the nanoparticle surface in the form of CoO_x during the CO oxidation reaction, and CO at high temperatures led to the migration of Pd to the surface. Further studies showed that this synergy could be further optimized by adjusting the ratio of Co/Pd, and the results showed that $Co_{0.24}Pd_{0.76}$ had the best CO conversion at low temperatures. Tofighi and coworkers synthesized bimetallic Au_xPd_y nanoparticles with different Au : Pd ratios and loaded them on TiO_2.[26] The strong electronic interactions existed between Au and Pd due to interatomic charge transfer and electronic modification in the d-bands of Au and Pd. In this bimetallic catalyst, Pd atoms adsorb and activate O_2 molecules, while CO is adsorbed at both Au and Pd sites, and the synergistic interaction between Pd and Au atoms results in the highest catalytic activity in CO oxidation over the Au_3Pd_7/TiO_2 catalyst. Choi *et al.* studied the influence of hydrothermal treatment on the activity of Pd-based bimetallic (Pd–Fe, Pd–Ni, and Pd–Co) catalysts deposited on CeO_2.[27] The hydrothermal treatment promoted the dispersion of Pd atoms and enhanced the interactions between Pd atoms and transition metals, which

in turn improved the CO oxidation activity, resulting in the $PdFe/CeO_2$-HT catalysts showing the highest catalytic activity. Grabow and co-workers examined the activity of PdCu alloy in CO oxidation.[75] As shown in Fig. 3b, the CO oxidation activity was correlated to the binding energy of O and CO. It was predicted that $PdCu_3$ alloys display comparable CO oxidation activity as that of PdPt. The $PdCu_3$ was able to achieve full oxidation of CO below 150 °C even in the presence of H_2O.

3.3 Effect of particle size

Soni and coworkers loaded small-sized (about 1 nm) Pd nanoparticles on SBA-15 by a modified deposition precipitation method.[28] The readily decomposable high-valent PdO_x species were present on the ligand-unsaturated Pd sites (Pd_{cus}) over smaller Pd nanoparticles. The weaker adsorption of CO on the small-sized Pd nanoparticles promoted the low-temperature CO oxidation activity. The CO oxidation mechanism on two different sizes of Pd nanoparticles was illustrated in Fig. 3e and f. Mehar and coworkers investigated the CO oxidation capacity of catalysts prepared by depositing Pd on ordered monolayer AgO_x/Ag (111) surfaces to probe the transfer of oxygen from AgO_x to Pd and how the size of the Pd clusters affects the oxygen transfer process.[77] The results showed that the high oxygenophilicity of Pd induced the transfer of oxygen atoms from AgO_x to Pd. The smaller the Pd cluster size, the more efficient the oxygen transfer and the higher the CO oxidation activity. The asymmetric edge sites of the Pd clusters had higher oxygen concentrations, which in turn led to a higher CO oxidation rate near the interface of Pd and AgO_x. Liu and co-workers reported that the transformation of Pd nanoclusters to nanoparticles occurred in the gas containing CO and H_2O.[53] As displayed in Fig. 3c, CO adsorbed on positively charged Pd species were observed when only CO was injected to the *in situ* cell in DRIFTS. On the other hand, when both CO and H_2O were injected, CO adsorbed on metallic Pd were identified indicating the transformation of highly dispersed Pd to nanoparticles (Fig. 3d).

4 Au-based catalysts

Bulk Au with filled d-orbital electrons showed lower activity for O_2 activation and therefore displayed lower oxidation activity.[78,79] However, when the Au particle downsized to the nanoscale, it showed excellent CO oxidation performance.[80–85] Current studies on Au-based catalysts focused on the effect of metal dopants, supported carriers, and water molecules on CO oxidation performance.

4.1 Effect of dopant

Doping components have been justified as an effective strategy to boost the CO oxidation performance of Au-based catalysts. Calzada *et al.* prepared bimetallic $AuRu/TiO_2$ catalysts by urea deposition precipitation and investigated their synergistic effect in CO oxidation.[86] The activity evaluation results indicated that the bimetallic catalysts displayed higher activity than Au/TiO_2. The $Au–Rh/TiO_2$ catalysts prepared by Camposeco *et al.* exhibited superior performance to monometallic catalysts. The results indicated that in the bimetallic system new CO adsorption sites were constructed, thereby improving the performance of the catalyst.[29] Wang *et al.* modified silica-loaded Au nanoparticle catalysts with CeO_x nanoparticles.[30] The CeO*x* nanomodification significantly boosted the concentration of $Au^{\delta+}$ on the surface of Au nanoparticles, leading to better activity and stability of CeO_x@ Au/SiO_2 catalysts than Au/SiO_2. Manzorro *et al.* prepared CeO_2-modified $Au/Y_2O_3–ZrO_2$ catalysts and elaborated that an atomic layer thickness of CeO_2 was generated on the surface of $Y_2O_3–ZrO_2$ microcrystals. This strengthened the interactions between CeO_2 and the loaded metal, and improved the CO oxidation activity and stability of the catalysts at high temperatures.[87] Boukha *et al.* investigated the CO oxidation performance of La-modified Au/HAP catalysts under hydrogen-enriched conditions.[31] The results showed that Au species existed in the form of $Au^{\sigma+}$ and Au^{+} after La doping. The addition of La boosted the chemisorption of CO and weakened the interaction of the catalyst with H_2 and H_2O, while the reducibility and oxygen mobility of the catalyst were also enhanced. The catalyst with the highest content of La (Au/La(6.6)/HAP) exhibited a CO conversion of 100% and the widest active temperature range.

4.2 Effects of carriers

The properties of the carrier have been proven to influence the CO oxidation performance of the Au-based catalysts. Mochizuki *et al.* synthesized Au_1/NiO catalysts and investigated the relationship between the surface state of NiO and the stability of Au monoatoms.[88] The experimental results indicated that Au monoatoms were more prone to be anchored on the surface of NiO with Ni vacancies than on the original NiO. Au atoms were positively charged on the NiO surface and their charge state depended on the carrier crystal structure. In addition, Au_1/NiO displayed high catalytic stability for CO oxidation reactions. Campbell *et al.* explored the relationship between the CO oxidation activity of Au/TiO_2 catalysts and the nature of the titanium dioxide carriers.[89] The amorphous TiO_2 carriers exhibited better activity than crystalline TiO_2 due to the presence of more active sites. Qi *et al.* deposited Au nanoparticles on Cu_2O nanoparticles with different morphologies and investigated the CO oxidation performance of the prepared catalysts under hydrogen-rich and oxygen-rich conditions.[32] The Au atoms were mainly adsorbed on the surface of Cu_2O, which did not change its initial morphology and the crystal structure. The results also revealed that Au nanoparticles smaller than 10 nm were deposited on the CuO surface with a strong interaction, which boosted the activity of the Au/CuO catalyst. Furthermore, Lin *et al.* prepared Au-deposited Ta_2O_5 catalysts with different crystalline structures (hexagonal, rhombohedral, and pyrochlore).[90] The results demonstrated that the Au-loaded hexagonal Ta_2O_5 (TT-Ta_2O_5) synthesized by the hydrothermal method possessed the highest CO oxidation activity. Further research revealed that the differences in the catalytic activity of CO oxidation were mainly attributed to the differences in oxygen activation and adsorption capacity of CO when Au was loaded

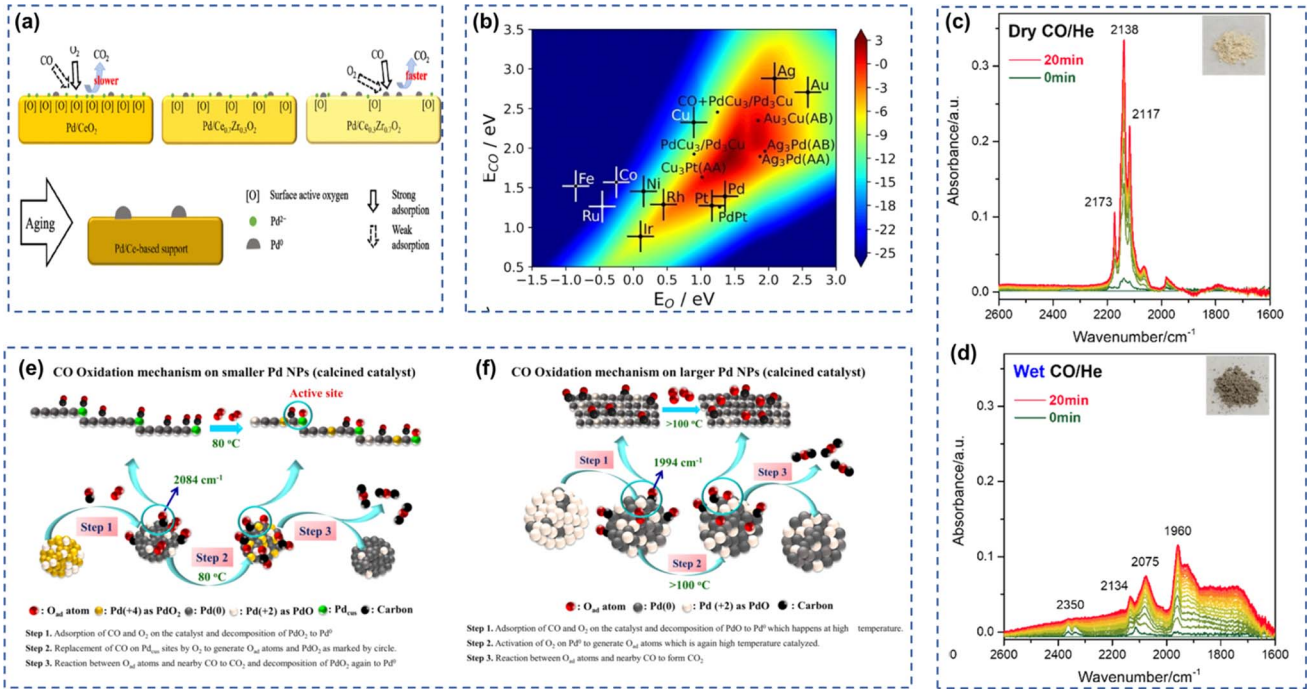

Fig. 3 (a) The scheme of CO oxidation on Pd/CeO_2, Pd/$Ce_{0.7}Zr_{0.3}O_2$ and Pd/$Ce_{0.3}Zr_{0.7}O_2$ catalysts. Reproduced with permission from ref. 10 Copyright 2020, American Chemical Society. (b) CO oxidation rate contour plot as a function of the binding energy of O and CO. Reproduced with permission from ref. 75 Copyright 2024, Wiley-VCH GmbH. DRIFTS spectra while flowing (c) CO/He and (d) CO + H_2O/He on Pd/FER. Reproduced with permission from ref. 71 Copyright 2023, American Chemical Society. The proposed scheme of CO oxidation on (e) small and (f) large Pd nanoparticles. Reproduced with permission from ref. 28 Copyright 2020, Elsevier.

on carriers with different crystal structures. Liu and co-workers reported the geometric edge effect on the interface of Au/CeO_2 in CO oxidation.[81] Au nanoparticles were dispersed on CeO_2 with various morphologies including cube, octahedron, and nanorod, among which nanorod CeO_2 showed the highest CO oxidation activity due to the unsaturated coordination environment, thus lowering the oxygen formation energy and promoting the CO adsorption (Fig. 4a–f). Similarly, Au nanoparticles were also anchored on ZnO nanorod or nanopyramid for CO oxidation.[79] Au loaded on ZnO nanorod showed a lower activation energy, thus displaying a higher CO oxidation activity (Fig. 4g and h).

4.3 The effect of water

H_2O has a significant effect on the catalytic oxidation activity of CO oxidation. To clarify the role of H_2O on CO oxidation performance on Au/TiO_2 catalyst at low temperatures, Fujitani *et al.* first deposited Au nanoparticles on the surface of single-crystal TiO_2(110), adsorbed H_2O to saturation, and then conducted a temperature-programed desorption analysis.[91] Two desorption peaks were observed in the H_2O-TPD spectrum: the peak at 370 K was attributed to molecular desorption of H_2O, while the peak at 510 K was attributed to recombinative desorption of H_2O. H_2O dissociated into H and OH at the interface of Au and TiO_2, and H_2O dissociation and CO oxidation were carried out at the same active sites. The authors claimed that the dissociation of H_2O triggered the oxidation of CO. Tran-Thuy *et al.* also investigated the effect of adsorbed H_2O molecules on the CO oxidation over Au/BN catalysts that were calcined at different temperatures.[92] The results showed that an increase in calcination temperature promoted the dispersion of Au particles on BN carriers. Besides, the high calcination temperature also improved the adsorption of water molecules on the surface, increased the defect density on the BN carriers, and enhanced the CO oxidation activity at room temperature and higher relative humidity conditions. The CO oxidation activity over the Au/BN catalysts increased with increasing relative humidity, and the TOF of the reaction at high humidity was correlated with physically adsorbed H_2O in a volcano-shape relationship with the adsorption intensity and the density of H_2O adsorbed on the surface. The increase in TOF under high humidity conditions could be attributed to the formation of $CO(H_2O)_n$ and H_2O_{ad} species, in which $CO(H_2O)_n$ was generated by CO_{ad} on Au^0 and H_2O_{ad} on BN, indicating the importance of the Au–BN interface sites. Zhao *et al.* also studied the promotion effect of H_2O on the oxidation activity of CO.[93] Compared to Au nanoparticles loaded on CeO_2 (Au/CeO_2-NP), water significantly affected the catalytic performance of Au single-atom catalysts (Au_1/CeO_2). In the Au_1/CeO_2 single-atom catalysts, the positively charged Au atoms as electron acceptors provided a more effective active site for the reaction of CO and OH groups due to their higher oxidation state change. On the other hand, the near zero-valent Au interfacial atoms in the supported Au nanoparticle catalysts were not conducive to this oxidation reaction, thus significantly hindering the CO + OH reaction pathway.

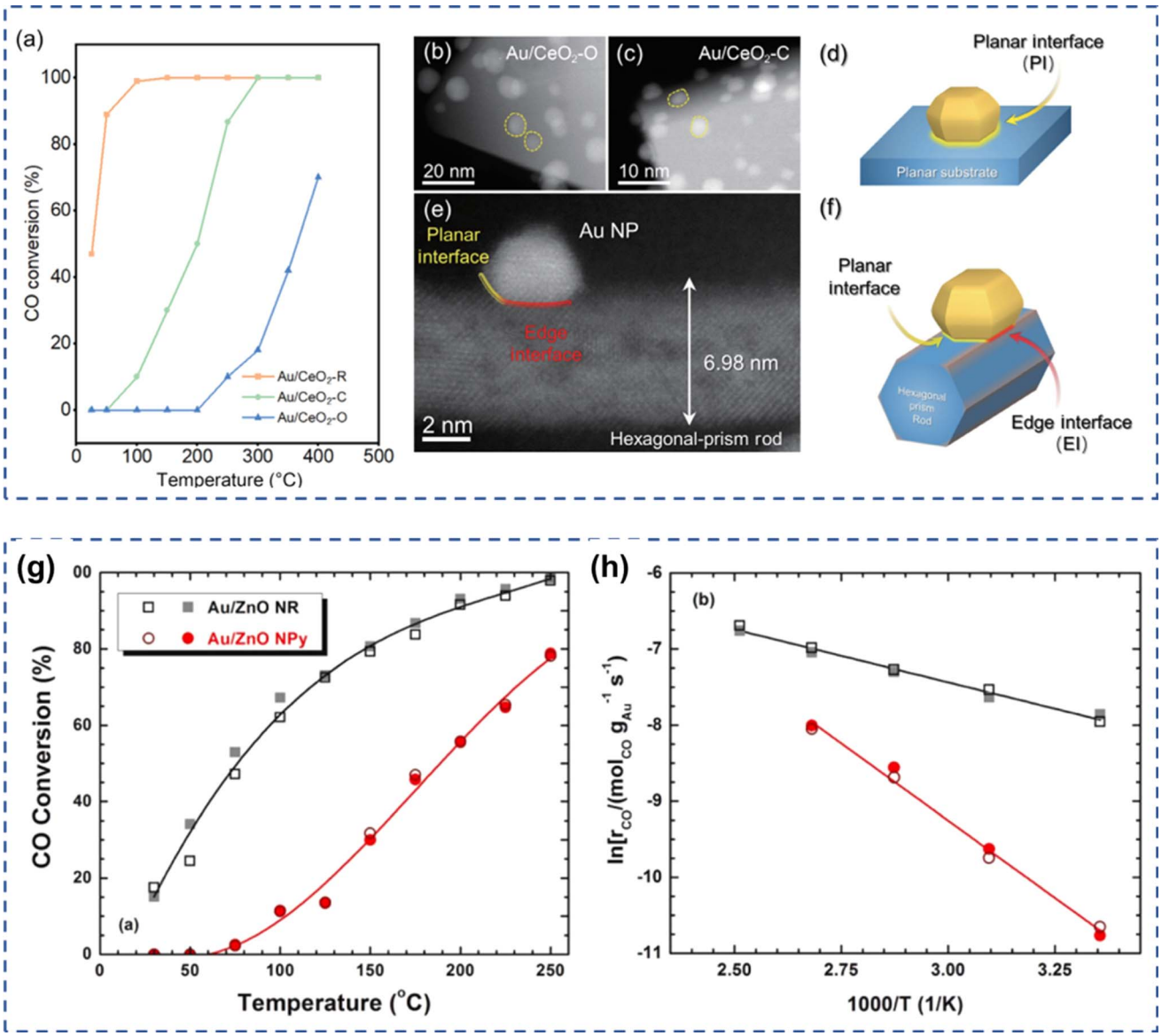

Fig. 4 (a) The CO oxidation performance over Au nanoparticles dispersed on various CeO_2. The TEM images of Au dispersed on (b) octahedron, (c) cube, and (e) nanorod. The scheme of (d) planar and (f) edge interface. Reproduced with permission from ref. 81 Copyright 2024, Springer. (g) The activity of CO oxidation and apparent activation (h) energy barrier for Au dispersed on ZnO nanorod and nanopyramid. Reproduced with permission from ref. 79 Copyright 2023, Elsevier.

5 Ru-based catalysts

Though Ru was less applied in CO oxidation compared to Au, Pt, and Pd-based catalysts, the effect of supports and metal doping on the catalytic performance of Ru-based catalysts was also reported in the literature.

5.1 Effects of supports

The nature of the carrier significantly affected the catalytic CO oxidation performance of Ru-based catalysts. Mohamed *et al.* investigated the CO oxidation over Ru/TiO_2 and Ru/ZrO_2 catalysts, and the results showed that the $Ru–ZrO_2$ catalysts were more active.[11] Zhang and co-workers prepared CeO_2 nanorod and nanocube *via* a hydrothermal method and examined the effect of CeO_2 morphology on Ru nanoparticles for CO oxidation (Fig. 5a).[94] Similarly, Li *et al.* designed and synthesized Ru catalysts loaded on CeO_2 nano-rods (NR), nano-cubes (NC), and nano-octahedra (NO) to investigate the effect between the shape and exposed crystalline surfaces ((100), (110), and (111)) of the nano-CeO_2 carriers on their low-temperature CO oxidation activity.[33] As shown in Fig. 5b–e, the (111) face of CeO_2 nanorods had a higher number of defects, while the nano-cubes and octahedra were surrounded by relatively flat (111) and (100) faces, respectively. The strong metal-support interaction between CeO_2 nanorods and RuO_x species rendered RuO_x to exhibit high stability in CO oxidation reactions. Ru^{n+} species were dominated in the $5Ru/CeO_2$ NR-r catalyst, and those

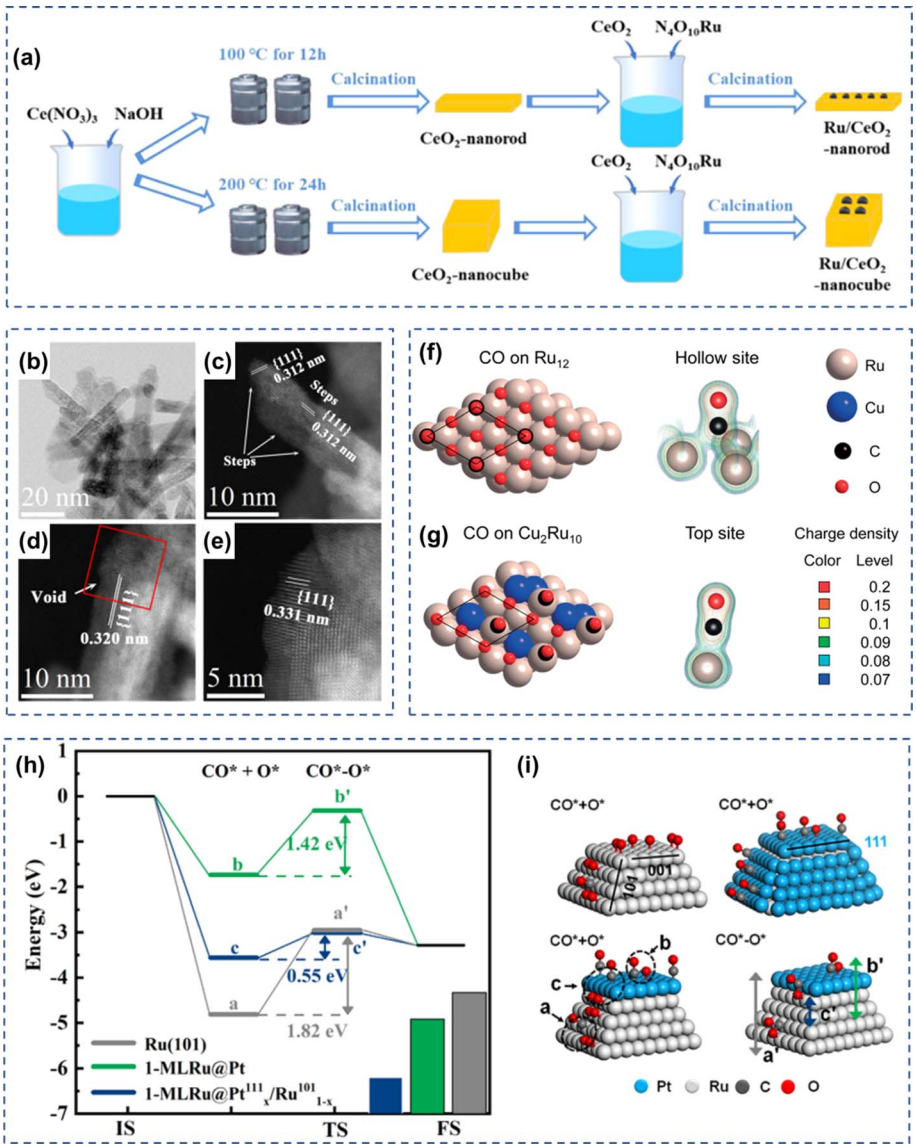

Fig. 5 (a) The illustration for the preparation of Ru/CeO_2. Reproduced with permission from ref. 94 Copyright 2022, American Chemical Society. (b) Low-magnification TEM image and (c and d) HAADF-STEM images of Ru/CeO_2NR catalyst after reduction treatment; (e) the enlarged image of the red square shown in (d). Reproduced with permission from ref. 33 Copyright 2019, American Chemical Society. CO adsorption models on (f) $Ru_{12}(111)$ and (g) Cu_2Ru_{10} surface. Reproduced with permission from ref. 34 Copyright 2019, Wiley. (h) The reaction energy barrier and (i) CO adsorption model on Ru(101), 1-MLRu@Pt, and 1-ML $Ru@Pt^{(111)}_x/Ru^{(101)}_{1-x}$ catalyst. Reproduced with permission from ref. 95 Copyright 2021, Elsevier.

species could diffuse into the surface lattice and form a Ru–O–Ce structure on the surface of CeO_2 nanorods, promoting the formation of oxygen vacancies. Therefore, CeO_2 nanorods-loaded Ru catalysts exhibited the strongest Ru–CeO_2 interactions, as well as strong reducibility and the highest low-temperature CO oxidation activity. Qin *et al.*[94] loaded Ru onto CeO_2 nano-rods (NR) and CeO_2 nano-cubes (NC) to investigate the effect of Ru–CeO_2 interaction on CO oxidation activity. The results showed that the interaction of Ru with CeO_2-NC was stronger than that with CeO_2-NR, which promoted the activation of lattice oxygen on CeO_2-NC while weakening the redox ability of RuO_x. The moderate interaction of Ru with CeO_2-NR resulted in a high redox capacity of RuO_x but a weak lattice oxygen activation ability of CeO_2-NR. Thus, the Ru/CeO_2-NR catalyst exhibited higher catalytic activity than Ru/CeO_2-NC in low-temperature CO oxidation reactions.

5.2 Elemental doping

Elemental doping also significantly affected the CO oxidation performance of Ru-based catalysts. Du *et al.* selectively deposited Pt on the (001) facet of Ru while exposing adjacent Ru surfaces by selective atomic layer deposition.[95] As shown in Fig. 5h and i, for the bifunctional faceted Pt/Ru catalysts, the deposition of a single layer of Pt atoms on Ru (001) effectively reduces the competitive adsorption of CO and lowers the

reaction barriers; and the neighboring exposed Ru surfaces have higher dissociation activity of O_2, which in turn improves the catalytic performance of the catalysts in the reaction. Huang *et al.* synthesized Cu_xRu_{1-x} solid solution alloyed nanoparticles, and the CO oxidation activity of Cu_xRu_{1-x} nanoparticles (x = 0.05–0.7) were all enhanced compared to Ru nanoparticles, and the highest CO oxidation activity was observed for $Cu_{0.2}Ru_{0.8}$ nanoparticles (Fig. 5f–g).[34] The Ru atoms in the Cu_xRu_{1-x} nanoparticles mainly acted as the active sites, and the Cu atom alloying attenuates the adsorption energy of CO on Ru atoms, thus enhancing the CO oxidation activity of Cu_xRu_{1-x} nanoparticles.

6 Rh-based catalysts

The catalyst carrier affects the effectiveness of CO oxidation on Rh-based catalysts. Rafaj *et al.* investigated the oxygen exchange properties between Rh nanoparticles and the carriers $CeO_2(111)$ or $CeO_2(110)$ in CO oxidation.[96] In a low-pressure reaction cycle at 300–770 K, the CO_2 produced by $Rh/CeO_2(111)$ and $Rh/CeO_2(110)$ contained 53% and 70% oxygen atoms originating from the carriers, respectively, and the oxygen mobility of $CeO_2(110)$ was higher than that of $CeO_2(111)$. The CO desorption energy of $Rh/CeO_2(111)$ was $2.39(7) \times 10^{-19}$ J and that of $Rh/CeO_2(110)$ was $2.28(7) \times 10^{-19}$ J. The catalytic performance of $Rh/CeO_2(110)$ was better due to the weaker CO–Rh bonding and higher oxygen exchange activity of the catalyst. González Vargas *et al.* synthesized 1 wt% Rh/Ce-MCM-41 catalyst using mesoporous Ce-MCM-41 material as a carrier.[35] In this catalyst, the small particle size of Rh and its high dispersion on the carrier surface, as well as the presence of silica hydroxyl groups on the catalyst surface would produce a synergistic effect, which enabled the Rh/Ce-MCM-41 catalyst to realize the complete conversion of CO at temperatures close to 440 K, whereas the reference samples Rh/CeO_2 and Rh/MCM-41 were inactive at this temperature. The mechanistic study of the low-temperature CO oxidation reaction of Rh/Ce-MCM-41 showed that CO adsorbed on Rh^{3+} clusters to form intermediate species, and Ce^{4+} doped in the mesoporous MCM-41 silica structure, along with an abundance of O–OH reactive oxygen species on the surface. Lin *et al.* deposited $CaTiO_3$ with a thickness of 1 nm on $MgAl_2O_4$ by atomic layer deposition, $SrTiO_3$ and $BaTiO_3$ films with a thickness of 1 nm on $MgAl_2O_4$, and investigated their CO catalytic oxidation performance as catalyst carriers loaded with Rh.[97] The interaction strengths of Rh with the three chalcogenide films followed the order of $Rh/CaTiO_3/MgAl_2O_4$ > $Rh/SrTiO_3/MgAl_2O_4$ > $Rh/BaTiO_3/MgAl_2O_4$. When Rh was loaded on

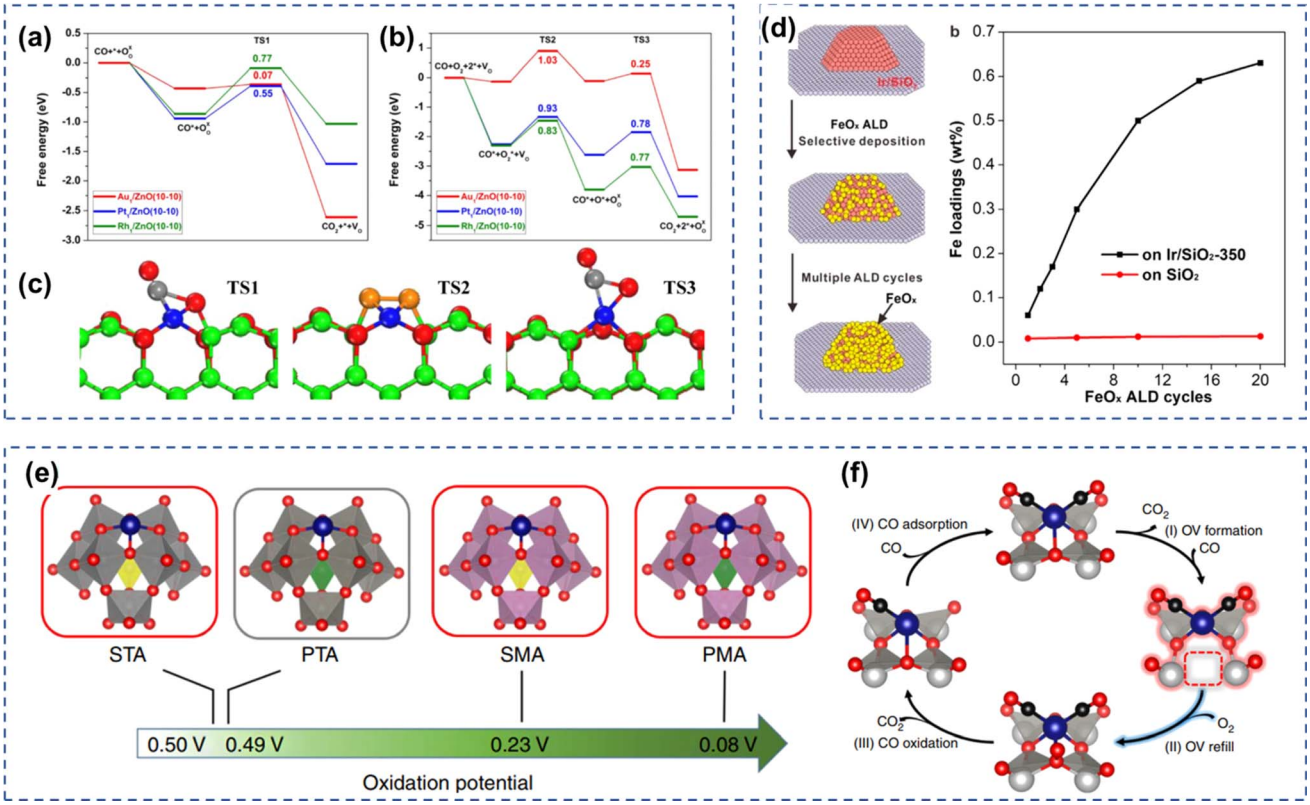

Fig. 6 (a and b) The free energy of CO oxidation *via* the M–vK mechanism over Rh_1/ZnO, Pt_1/ZnO, and Au_1/ZnO SACs catalysts, respectively; (c) the optimized state of the elementary step in CO oxidation, where the green, blue, red, orange, and gray balls represent Zn Rh/Pt/Au, O, O from O_2, and C atoms, respectively. Reproduced with permission from ref. 8 Copyright 2019, Elsevier. (d) The effect of FeO_x ALD cycling on the activity of Ir in CO oxidation. Reproduced with permission from ref. 36 Copyright 2019, American Chemical Society. (e) The oxidation potential of single-atom Rh dispersed on four heteropoly acids. (f) The proposed reaction mechanism of CO oxidation over single-atom Rh anchored on heteropoly acid. Reproduced with permission from ref. 98 Copyright 2019, Nature Publishing Group.

$MgAl_2O_4$ or $BaTiO_3$ films, Rh species formed larger particles after redox cycling at 1073 K, but small particles were formed on $SrTiO_3$ films and remained better atomically dispersed on $CaTiO_3$ films. $Rh/SrTiO_3/MgAl_2O_4$ showed strong oxidizing activity for CO after reduction at 1073 K, while $Rh/CaTiO_3/MgAl_2O_4$ showed low oxidizing activity for CO. Rh monoatomic catalysts also showed high reactivity for CO oxidation. Han *et al.* prepared Rh, Au and Pt monoatomic catalysts with ZnO nanowires (ZnO-nw) as carriers and studied their CO oxidation performance.[8] As shown in Fig. 6a–c, the reaction proceeds following the Mars-van Krevelen mechanism and the dissociation of oxygen molecules at the surface oxygen vacancies is the rate-controlling step of the reaction. Among the three noble metals studied, the Rh1/ZnO-nw catalysts have the lowest energy barriers, and thus they have the highest CO oxidation activity, and the Rh1/ZnO-nw catalysts have better resistance to high-temperature sintering. Hulsey *et al.* explored the active center of Rh-HPA catalysts in CO oxidation and demonstrated that atomically dispersed Rh-catalyzed CO oxidation follows an unconventional M–vK mechanism and that heteropolyacid carriers are directly involved in the reaction Fig. 6e–f.[98] Rh cycles between Rh^{3+} and Rh^{+} and the reoxidation of the carrier is a rate-controlling step.

7 Ir-based catalysts

Hong *et al.* used Fe-substituted hexaaluminate as a support to disperse Ir nanoparticles ($Ir/BaFeAl_{11}O_{19}$) for CO oxidation.[9] The interaction between Ir species on the crystalline surface of hexaaluminate and the Fe species in the matrix of support resulted in Fe oxidation state of +2, and the moderate adsorption of CO on the Ir sites, thus the catalyst showed good catalytic performance in the CO-PROX reaction with high conversion, good stability, and strong resistance to CO_2 and H_2O poisoning. Wang *et al.* adopted atomic layer deposition strategies to selectively deposit FeO_x onto SiO_2 and then further loaded Ir nanoparticles with different particle sizes (Fig. 6d).[36] The activity of FeO_x-coated Ir/SiO_2 samples was significantly higher compared to the uncoated Ir/SiO_2 samples and showed a volcano-shaped pattern as the number of FeO_x deposition cycles increased. Among them, the 1.5 nm Ir/SiO_2 sample showed the best catalytic performance by achieving the complete conversion of CO in a wide temperature range of 60–180 °C after two FeO_x cycles.

8 Conclusion and outlook

With the development of modern industry, the negative effect of CO on the environment is becoming more and more serious. CO catalytic oxidation is an effective approach to reducing CO. Noble metal catalysts have been widely used for CO catalytic oxidation due to their better catalytic performance. Most of the current studies focused on the influences of elemental doping, the particle size of precious metals, carrier type, oxygen vacancies, and surface hydroxyl groups on CO catalytic oxidation. Despite the tremendous progress has been made in the design and fabrication of noble metal-based catalysts for CO oxidation, the practical application of those catalysts still faces some problems and challenges that can not be ignored. In this section, the challenges and opportunities in the development of efficient catalysts for CO oxidation will be offered.

(1) The stability and poisoning resistance of noble metal-based catalysts still need to be improved. The composition of the exhaust gases is complex, containing a certain percentage of water vapor and SO_2, *etc.* It was widely accepted that the SO_2 poisoned and deactivated the noble metal-based catalysts to form sulfate or sulfite. The development of precious metal catalysts with high SO_2 poisoning resistance is urgent. One of the possible strategies is to coat the noble-metal catalysts with a thin layer of acidic metal oxides, which suppressed the adsorption of SO_2, thus protecting the noble-metal sites from poisoning. Considering that the size of CO is smaller than SO_2, the other possible approach was to the confine the noble-metal atoms within the small size pore of the zeolites, in which the pore only allowed the adsorption of CO on metal sites, and protected the noble metals from interacting with SO_2. Other strategies to enhance the SO_2 resistance are still highly desirable. Besides, the methods to regenerate the poisoned catalysts are also needed.

(2) The design and selection of catalytic materials are the key to efficiently remove CO. Though noble metal-based catalysts were demonstrated effective, the high price limits the large application of noble metals. The cost of precious metals accounts for more than 90% of the catalyst production. How to reduce the loading of precious metals without compromising the catalytic performance is the focus of the research. Thanks to the emergence of single-atom catalysts, which were characterized by the 100% exposure of the metal atoms, the effective removal of CO molecules with acceptable cost is becoming possible. On the other hand, non-noble metal catalysts with comparable catalytic performance as noble metal catalysts are more desirable. The transition metal nitride and carbide behave like noble metals in electrochemical reactions, such as the oxygen reduction reactions, and the hydrogen evolution reactions. The application of transition metal nitride and carbide in CO might be able to further decrease the cost of the catalysts. It should be noted that the metal nitride/carbide could be oxidized to metal oxides under oxygen-rich conditions. The formed metal nitride@oxide structure might possess unique electronic and geometric properties that enable effective CO oxidation.

(3) The active sites of CO oxidation over noble metal-based catalysts were still ambiguous. Some research reported that atomically dispersed metal species were responsible for the CO oxidation, while it was also claimed that the nanoclusters were the sites where the reaction occurred. The current techniques to identify the single-atom sites heavily rely on HAADF-STEM, XAFS, and DRIFTS. Though those techniques can provide the general structure information of the sample, it is still challenging to precisely reveal the electronic and coordination environment with spatial resolution under working conditions. Besides, a wide range of metal particle sizes were present in the heterogeneous catalysts. It is challenging to distinguish the real active sites.

(4) Apart from studying the structure of the catalysts, it is also critical to investigate the reaction mechanism as well as the structure–performance relationship under working conditions. The understanding of the reaction mechanism and the structure–performance relationship are the cornerstone for the development of efficient CO oxidation catalysts. Although enormous progress has been made in the mechanism study, most of the studies were carried out under ideal conditions. How the molecules such as H_2O and SO_2 that are generally present in the exhaust affected the reaction mechanism still needs to be further investigated. Besides, theoretical calculation combined with experimental measurement is another area to explore.

(5) Artificial intelligence should be applied in the design of CO oxidation catalysts. Artificial intelligence is playing a more and more important role in catalysis. The rapid development of both the hardware and software makes it possible to acquire a huge amount of catalysis data, including reaction rate, kinetic behavior, and the *operando* spectroscopy. All the information can help to predict the CO oxidation activity of a particular catalyst. On the other hand, the machine learning-based technique enables the discovery of the key descriptors, such as work function, d-band center and Fermi energy, governing the CO oxidation reaction rate. Based on the descriptor, we can design a catalyst with excellent CO oxidation activity. We also expected that the research along this line will promote the identification of the best catalysts in CO oxidation.

Data availability

No primary research results, software or code have been included and no new data were generated or analysed as part of this review.

Conflicts of interest

The authors declare that they have no known competing financial interests or personal relationships that could have appeared to influence the work reported in this paper.

Acknowledgements

This work is supported by the Open Project Program of the State Key Laboratory of Clean and Efficient Coal-Fired Power Generation and Pollution Control (D2022FK093). The authors also would like to acknowledge the Natural Science Foundation of Jiangsu Province (BK20220847) for the financial support.

References

1 P. Chai, Z. Wu, L. Wu, H. Wang, C. Fu and W. Huang, An Operando Study of H_2O-Enhanced Low-Temperature CO Oxidation on Pt(111) under Near Ambient Pressure Conditions, *ACS Catal.*, 2022, 13292–13299.

2 C. A. Whitcomb, A. Shrestha, C. Paolucci and R. J. Davis, Low temperature CO oxidation over Rh supported on N-doped carbon, *Catal. Sci. Technol.*, 2024, 2479–2488.

3 X. Mao, Y. Zhang, Y. Xu, Y. Zhou, K. Zhuang, K. Shen and S. Ding, The lattice oxygen determines the methanol selectivity in CO_2 hydrogenation over $ZnZrO_x$ catalysts, *Catal. Sci. Technol.*, 2024, **14**(2), 419–430.

4 L. Xiang, S. Wang and L. Kuai, Superior single-atom Pt/TiO_2 mesoporous microspheres via microdrops-confined pyrolysis/deposition for low-temperature CO oxidation, *Microporous Mesoporous Mater.*, 2024, **363**, 112809.

5 Z. Cui, X. Wang, R. Li, L. Kuai and C. Fang, Spatially confined (Au core)/CeO_2–(Au nanoclusters) hierarchical nanostructures as highly active and stable catalysts for CO oxidation, *J. Alloys Compd.*, 2023, **938**, 168655.

6 C. Fang, X. Jiang, J. Hu, J. Song, N. Sun, D. Zhang and L. Kuai, Ru Nanoworms Loaded TiO(2) for Their Catalytic Performances toward CO Oxidation, *ACS Appl. Mater. Interfaces*, 2021, **13**(4), 5079–5087.

7 Y. Chen, Y. Feng, L. Li, J. Liu, X. Pan, W. Liu, F. Wei, Y. Cui, B. Qiao, X. Sun, X. Li, J. Lin, S. Lin, X. Wang and T. Zhang, Identification of Active Sites on High-Performance Pt/Al2O3 Catalyst for Cryogenic CO Oxidation, *ACS Catal.*, 2020, **10**(15), 8815–8824.

8 B. Han, R. Lang, H. Tang, J. Xu, X.-K. Gu, B. Qiao and J. Liu, Superior activity of Rh1/ZnO single-atom catalyst for CO oxidation, *Chin. J. Catal.*, 2019, **40**(12), 1847–1853.

9 B. Hong, J.-X. Liang, X. Sun, M. Tian, F. Huang, Y. Zheng, J. Lin, L. Li, Y. Zhou and X. Wang, Widening Temperature Window for CO Preferential Oxidation in H_2 by Ir Nanoparticles Interaction with Framework Fe of Hexaaluminate, *ACS Catal.*, 2021, **11**(9), 5709–5717.

10 H. Li, M. Shen, J. Wang, H. Wang and J. Wang, Effect of Support on CO Oxidation Performance over the Pd/CeO_2 and Pd/CeO_2–ZrO_2 Catalyst, *Ind. Eng. Chem. Res.*, 2020, **59**(4), 1477–1486.

11 Z. Mohamed, V. D. B. C. Dasireddy, S. Singh and H. B. Friedrich, TiO_2 and ZrO_2 supported Ru catalysts for CO mitigation following the water-gas shift reaction, *Int. J. Hydrogen Energy*, 2018, **43**(49), 22291–22302.

12 C. Feng, X. Liu, T. Zhu and M. Tian, Catalytic oxidation of CO on noble metal-based catalysts, *Environ. Sci. Pollut. Res. Int.*, 2021, **28**(20), 24847–24871.

13 Z. Jia, M. Peng, X. Cai, Y. Chen, X. Chen, F. Huang, L. Zhao, J. Diao, N. Wang, D. Xiao, X. Wen, Z. Jiang, H. Liu and D. Ma, Fully Exposed Platinum Clusters on a Nanodiamond/Graphene Hybrid for Efficient Low-Temperature CO Oxidation, *ACS Catal.*, 2022, 9602–9610.

14 J. Cai, Z. Yu, X. Fan and J. Li, Effect of TiO(2) Calcination Pretreatment on the Performance of Pt/TiO(2) Catalyst for CO Oxidation, *Molecules*, 2022, **27**(12), 3875.

15 F. Maurer, A. Beck, J. Jelic, W. Wang, S. Mangold, M. Stehle, D. Wang, P. Dolcet, A. M. Gaenzler, C. Kuebel, F. Studt, M. Casapu and J.-D. Grunwaldt, Surface Noble Metal Concentration on Ceria as a Key Descriptor for Efficient Catalytic CO Oxidation, *ACS Catal.*, 2022, **12**(4), 2473–2486.

16 S. Song, Y. Wu, S. Ge, L. Wang, Y. Wang, Y. Guo, W. Zhan and Y. Guo, A Facile Way To Improve Pt Atom Efficiency for CO Oxidation at Low Temperature: Modification by Transition Metal Oxides, *ACS Catal.*, 2019, **9**(7), 6177–6187.

17 B. Nan, Q. Fu, J. Yu, M. Shu, L.-L. Zhou, J. Li, W.-W. Wang, C.-J. Jia, C. Ma, J.-X. Chen, L. Li and R. Si, Unique structure of active platinum-bismuth site for oxidation of carbon monoxide, *Nat. Commun.*, 2021, **12**(1), 3342.

18 J. Bae, J. Kim, H. Jeong and H. Lee, CO oxidation on SnO2 surfaces enhanced by metal doping, *Catal. Sci. Technol.*, 2018, **8**(3), 782–789.

19 W. Wang, D. Li, H. Yu, C. Liu, C. Tang, J. Chen, J. Lu and M. Luo, Insights into Different Reaction Behaviors of Propane and CO Oxidation over Pt/CeO_2 and Pt/Nb_2O_5: The Crucial Roles of Support Properties, *J. Phys. Chem. C*, 2021, **125**(35), 19301–19310.

20 G. Spezzati, A. D. Benavidez, A. T. DeLaRiva, Y. Su, J. P. Hofmann, S. Asahina, E. J. Olivier, J. H. Neethling, J. T. Miller, A. K. Datye and E. J. M. Hensen, CO oxidation by Pd supported on CeO_2(100) and CeO_2(111) facets, *Appl. Catal., B*, 2019, **243**, 36–46.

21 E. M. Slavinskaya, A. V. Zadesenets, O. A. Stonkus, A. I. Stadnichenko, A. V. Shchukarev, Y. V. Shubin, S. V. Korenev and A. I. Boronin, Thermal activation of Pd/CeO_2–SnO_2 catalysts for low-temperature CO oxidation, *Appl. Catal., B*, 2020, **277**, 119275.

22 H. Xu, Z. Zhang, J. Liu, C. L. Do-Thanh, H. Chen, S. Xu, Q. Lin, Y. Jiao, J. Wang, Y. Wang, Y. Chen and S. Dai, Entropy-stabilized single-atom Pd catalysts via high-entropy fluorite oxide supports, *Nat. Commun.*, 2020, **11**(1), 3908.

23 L. Wang, C. Pu, L. Xu, Y. Cai, Y. Guo, Y. Guo and G. Lu, Effect of supports over Pd/Fe_2O_3 on CO oxidation at low temperature, *Fuel Process. Technol.*, 2017, **160**, 152–157.

24 C. Wang, C. Wen, J. Lauterbach and E. Sasmaz, Superior oxygen transfer ability of Pd/MnO_x–CeO_2 for enhanced low temperature CO oxidation activity, *Appl. Catal., B*, 2017, **206**, 1–8.

25 C. H. Wu, C. Liu, D. Su, H. L. Xin, H.-T. Fang, B. Eren, S. Zhang, C. B. Murray and M. B. Salmeron, Bimetallic synergy in cobalt–palladium nanocatalysts for CO oxidation, *Nat. Catal.*, 2018, **2**(1), 78–85.

26 G. Tofighi, X. Yu, H. Lichtenberg, D. E. Doronkin, W. Wang, C. Wöll, Y. Wang and J.-D. Grunwaldt, Chemical Nature of Microfluidically Synthesized AuPd Nanoalloys Supported on TiO_2, *ACS Catal.*, 2019, **9**(6), 5462–5473.

27 M. S. Choi, H. Jeong and H. Lee, Re-dispersion of Pd-based bimetallic catalysts by hydrothermal treatment for CO oxidation, *RSC Adv.*, 2021, **11**(5), 3104–3109.

28 Y. Soni, S. Pradhan, M. K. Bamnia, A. K. Yadav, S. N. Jha, D. Bhattacharyya, T. S. Khan, M. A. Haider and C. P. Vinod, Spectroscopic Evidences for the Size Dependent Generation of Pd Species Responsible for the Low Temperature CO Oxidation Activity on Pd-SBA-15 Nanocatalyst, *Appl. Catal., B*, 2020, **272**, 118934.

29 R. Camposeco, M. Hinojosa-Reyes, S. Castillo, N. Nava and R. Zanella, Synthesis and characterization of highly dispersed bimetallic Au-Rh nanoparticles supported on titanate nanotubes for CO oxidation reaction at low temperature, *Environ. Sci. Pollut. Res. Int.*, 2021, **28**(9), 10734–10748.

30 L. Wang, L. Wang, J. Zhang, H. Wang and F.-S. Xiao, Enhancement of the activity and durability in CO oxidation over silica-supported Au nanoparticle catalyst via CeO modification, *Chin. J. Catal.*, 2018, **39**(10), 1608–1614.

31 Z. Boukha, J. R. González-Velasco and M. A. Gutiérrez-Ortiz, Viability of Au/La2O3/HAP catalysts for the CO preferential oxidation reaction under reformate gas conditions, *Appl. Catal., B*, 2022, **312**, 121384.

32 C. Qi, Y. Zheng, H. Lin, H. Su, X. Sun and L. Sun, CO oxidation over gold catalysts supported on CuO/Cu_2O both in O_2-rich and H2-rich streams: Necessity of copper oxide, *Appl. Catal., B*, 2019, **253**, 160–169.

33 J. Li, Z. Liu, D. A. Cullen, W. Hu, J. Huang, L. Yao, Z. Peng, P. Liao and R. Wang, Distribution and Valence State of Ru Species on CeO_2 Supports: Support Shape Effect and Its Influence on CO Oxidation, *ACS Catal.*, 2019, **9**(12), 11088–11103.

34 B. Huang, H. Kobayashi, T. Yamamoto, T. Toriyama, S. Matsumura, Y. Nishida, K. Sato, K. Nagaoka, M. Haneda, W. Xie, Y. Nanba, M. Koyama, F. Wang, S. Kawaguchi, Y. Kubota and H. Kitagawa, A CO Adsorption Site Change Induced by Copper Substitution in a Ruthenium Catalyst for Enhanced CO Oxidation Activity, *Angew Chem. Int. Ed. Engl.*, 2019, **58**(8), 2230–2235.

35 O. A. González Vargas, J. A. de Los Reyes Heredia, V. A. Suarez-Toriello, S. M. Anderson, L. F. Chen and J. A. Wang, Enhanced catalytic performance of Ce-MCM-41-supported Rh for CO oxidation, *Res. Chem. Intermed.*, 2021, **47**(7), 2857–2880.

36 C. Wang, Q. Yao, L. Cao, J. Li, S. Chen and J. Lu, Precise Tailoring of Ir-FeOx Interfaces for Improved Catalytic Performance in Preferential Oxidation of Carbon Monoxide in Hydrogen, *J. Phys. Chem. C*, 2019, **123**(48), 29262–29270.

37 B. Qiao, A. Wang, X. Yang, L. F. Allard, Z. Jiang, Y. Cui, J. Liu, J. Li and T. Zhang, Single-atom catalysis of CO oxidation using Pt_1/FeO_x, *Nat. Chem.*, 2011, **3**(8), 634–641.

38 B. Qiao, J.-X. Liang, A. Wang, C.-Q. Xu, J. Li, T. Zhang and J. Liu, Ultrastable single-atom gold catalysts with strong covalent metal-support interaction (CMSI), *Nano Res.*, 2015, **8**(9), 2913–2924.

39 L. Jiao and J. R. Regalbuto, The synthesis of highly dispersed noble and base metals on silica via strong electrostatic adsorption: I. Amorphous silica, *J. Catal.*, 2008, **260**(2), 329–341.

40 Z. Zhang, Y. Zhu, H. Asakura, B. Zhang, J. Zhang, M. Zhou, Y. Han, T. Tanaka, A. Wang, T. Zhang and N. Yan, Thermally stable single atom $Pt/m\text{-}Al_2O_3$ for selective hydrogenation and CO oxidation, *Nat. Commun.*, 2017, **8**, 16100.

41 Z. Zhang, C. Feng, C. Liu, M. Zuo, L. Qin, X. Yan, Y. Xing, H. Li, R. Si, S. Zhou and J. Zeng, Electrochemical deposition as a universal route for fabricating single-atom catalysts, *Nat. Commun.*, 2020, **11**(1), 1215.

42 P. Liu, Y. Zhao, R. Qin, S. Mo, G. Chen, L. Gu, D. M. Chevrier, P. Zhang, Q. Guo, D. Zang, B. Wu, G. Fu and N. Zheng, Photochemical route for synthesizing atomically dispersed palladium catalysts, *Science*, 2016, **352**(6287), 797–801.

43 S. Ding, H.-A. Chen, O. Mekasuwandumrong, M. J. Hülsey, X. Fu, Q. He, J. Panpranot, C.-M. Yang and N. Yan, High-temperature flame spray pyrolysis induced stabilization of Pt single-atom catalysts, *Appl. Catal., B*, 2021, **281**, 119471.

44 M. Liebertseder, C. B. Maliakkal, M. Crone, G. Nails, M. Casapu, J.-D. Grunwaldt, M. Tuerk, C. Kuebel and C. Feldmann, TiO_2–CeO_x–Pt Hollow Nanosphere Catalyst for Low-Temperature CO Oxidation, *Chemcatchem*, 2024, **16**(2), e202301358.

45 C. Chen, J.-L. Chen, L. Feng, J. Hu, X. Chai, J.-X. Liu and W.-X. Li, Reactant-Induced Dynamic Stabilization of Highly Dispersed Pt Catalysts on Ceria Dictating the Reactivity of CO Oxidation, *ACS Catal.*, 2024, **14**(5), 3504–3513.

46 Z. Zhang, J. Tian, Y. Lu, S. Yang, D. Jiang, W. Huang, Y. Li, J. Hong, A. S. Hoffman, S. R. Bare, M. H. Engelhard, A. K. Datye and Y. Wang, Memory-dictated dynamics of single-atom Pt on CeO_2 for CO oxidation, *Nat. Commun.*, 2023, **14**(1), 2664.

47 L. Xu, Y. Pan, H. Li, R. Xu and Z. Sun, Highly active and water-resistant Lanthanum-doped platinum-cobalt oxide catalysts for CO oxidation, *Appl. Catal., B*, 2023, **331**, 122678.

48 H. J. Wallander, D. Gajdek, S. Albertin, G. Harlow, N. Braud, L. Buss, J.-O. Krisponeit, J. I. Flege, J. Falta, E. Lundgren and L. R. Merte, Dynamic Behavior of Tin at Platinum Surfaces during Catalytic CO Oxidation, *ACS Catal.*, 2023, **13**(24), 16158–16167.

49 I. V. Zagaynov, E. Y. Liberman and A. V. Naumkin, Influence of Pt/Pd state on ceria-based support in CO oxidation, *J. Rare Earths*, 2023, **41**(12), 1963–1968.

50 T. Ueda, T. Matsuo, T. Hyodo and Y. Shimizu, Effects of heat treatments of Pt-loaded Al_2O_3 on catalytic activities of CO oxidation and combustion-type CO sensors, *J. Mater. Sci.*, 2023, 9459–9472.

51 E. M. Slavinskaya, A. I. Stadnichenko, J. E. Q. Dominguez, O. A. Stonkus, M. Vorokhta, B. Smid, P. Castro-Latorre, A. Bruix, K. M. Neyman and A. I. Boronin, States of Pt/CeO_2 catalysts for CO oxidation below room temperature, *J. Catal.*, 2023, **421**, 285–299.

52 K. Shen, R. J. Gorte and J. M. Vohs, H_2O Promotion of CO Oxidation On Oxidized Pt/$CeFeO_x$, *Catal. Lett.*, 2023, 2414–2421.

53 X. Liu, Y. Zou, X. Li, T. Xu, W. Cen, B. Li and T. Zhu, Ultralow Doping of Mn Species into Pt Catalyst Enhances the CO Oxidation Performance in the Presence of H_2O and SO_2, *ACS Catal.*, 2023, **13**(22), 14580–14597.

54 Y. Li, H. Wang, H. Song, N. Rui, M. Kottwitz, S. D. Senanayake, R. G. Nuzzo, Z. Wu, D.-e. Jiang and A. I. Frenkel, Active sites of atomically dispersed Pt supported on Gd-doped ceria with improved low temperature performance for CO oxidation, *Chem. Sci.*, 2023, **14**(44), 12582–12588.

55 D. Kim, D. Park, H. C. Song, B. Jeong, J. Lee, Y. Jung and J. Y. Park, Metal Encapsulation-Driven Strong Metal-Support Interaction on Pt/Co_3O_4 during CO Oxidation, *ACS Catal.*, 2023, **13**(8), 5326–5335.

56 S. Hu, M. Huang, J. Li, J. He, K. Xu, X. Rao, D. Cai and G. Zhan, Tailoring the electronic states of Pt by atomic layer deposition of Al_2O_3 for enhanced CO oxidation performance: Experimental and theoretical investigations, *Appl. Catal., B*, 2023, **333**, 122804.

57 S. Hong, D. Kim, K.-J. Kim and J. Y. Park, Facet-Controlled Cu_2O Support Enhances Catalytic Activity of Pt Nanoparticles for CO Oxidation, *J. Phys. Chem. Lett.*, 2023, **14**(23), 5241–5248.

58 J. Dong, Y. Zhang, D. Li, A. Adogwa, S. Huang, M. Yang, J. Yang and Q. Jin, Reaction-driven evolutions of Pt states over Pt–CeO_2 catalysts during CO oxidation, *Appl. Catal., B*, 2023, **330**, 122662.

59 S. Dhakar, A. Sharma, N. K. Katiyar, A. Parui, R. Das, A. K. Singh, C. S. Tiwary, S. Sharma and K. Biswas, Utilization of structural high entropy alloy for CO oxidation to CO_2, *Mater. Today Energy*, 2023, **37**, 101386.

60 D. Wang, R. Li, X. Sun, L. Lin, K. Li, R. Zhang, R. Mu and Q. Fu, Hydroxide Structure-Dependent OH Promotion Mechanism over a Hydroxylated CoOx/Pt(111) Catalyst toward CO Oxidation, *ACS Catal.*, 2024, **14**(7), 5147–5155.

61 X. Wang, S. Zeng, G. Qi, Q. Wang, J. Xu and F. Deng, CO oxidation over embedded Pt nanoparticles on Al_2O_3 with Al coordination flexibility, *Chem. Commun.*, 2023, **59**(50), 7783–7786.

62 A. Beniya, S. Higashi, N. Ohba, R. Jinnouchi, H. Hirata and Y. Watanabe, CO oxidation activity of non-reducible oxide-supported mass-selected few-atom Pt single-clusters, *Nat. Commun.*, 2020, **11**(1), 1888.

63 Z. Jia, M. Peng, X. Cai, Y. Chen, X. Chen, F. Huang, L. Zhao, J. Diao, N. Wang, D. Xiao, X. Wen, Z. Jiang, H. Liu and D. Ma, Fully Exposed Platinum Clusters on a Nanodiamond/Graphene Hybrid for Efficient Low-Temperature CO Oxidation, *ACS Catal.*, 2022, **12**(15), 9602–9610.

64 C. Dessal, T. Len, F. Morfin, J.-L. Rousset, M. Aouine, P. Afanasiev and L. Piccolo, Dynamics of Single Pt Atoms on Alumina during CO Oxidation Monitored by Operando X-ray and Infrared Spectroscopies, *ACS Catal.*, 2019, **9**(6), 5752–5759.

65 J. Chen, S. Xiong, H. Liu, J. Shi, J. Mi, H. Liu, Z. Gong, L. Oliviero, F. Mauge and J. Li, Reverse oxygen spillover triggered by CO adsorption on Sn-doped Pt/TiO_2 for low-temperature CO oxidation, *Nat. Commun.*, 2023, **14**(1), 3477.

66 H. Wang, J. Dong, L. F. Allard, S. Lee, S. Oh, J. Wang, W. Li, M. Shen and M. Yang, Single-site Pt/La–Al_2O_3 stabilized by barium as an active and stable catalyst in purifying CO and C_3H_6 emissions, *Appl. Catal., B*, 2019, **244**, 327–339.

67 S. Lee, C. Lin, S. Kim, X. Mao, T. Kim, S.-J. Kim, R. J. Gorte and W. Jung, Manganese Oxide Overlayers Promote CO Oxidation on Pt, *ACS Catal.*, 2021, **11**(22), 13935–13946.

68 Y. Chen, J. Lin, L. Li, X. Pan, X. Wang and T. Zhang, Local structure of Pt species dictates remarkable performance on Pt/Al_2O_3 for preferential oxidation of CO in H-2, *Appl. Catal., B*, 2021, **282**, 119588.

69 H. Liu, A. Zakhtser, A. Naitabdi, F. Rochet, F. Bournel, C. Salzemann, C. Petit, J.-J. Gallet and W. Jie, Operando Near-Ambient Pressure X-ray Photoelectron Spectroscopy Study of the CO Oxidation Reaction on the Oxide/Metal

Model Catalyst ZnO/Pt(111), *ACS Catal.*, 2019, **9**(11), 10212–10225.

70 J. Cai, Z. Liu, K. Cao, Y. Lang, S. Chu, B. Shan and R. Chen, Highly dispersed Pt studded on CoOx nanoclusters for CO preferential oxidation in H2, *J. Mater. Chem. A*, 2020, **8**(20), 10180–10187.

71 I. Song, I. Z. Koleva, H. A. Aleksandrov, L. Chen, J. Heo, D. Li, Y. Wang, J. Szanyi and K. Khivantsev, Ultrasmall Pd Clusters in FER Zeolite Alleviate CO Poisoning for Effective Low-Temperature Carbon Monoxide Oxidation, *J. Am. Chem. Soc.*, 2023, **145**(50), 27493–27499.

72 H. Liu, S. Wu, C. Sun, Z. Huang, H. Xu and W. Shen, Fabricating Uniform TiO_2-CeO_2 Solid Solution Supported Pd Catalysts by an In Situ Capture Strategy for Low-Temperature CO Oxidation, *ACS Appl. Mater. Interfaces*, 2023, **15**(8), 10795–10802.

73 A. S. Khder, H. M. Altass, R. S. Jassas, M. M. Al-Rooqi, M. A. Khder, M. Morad, A. Gebreil, Z. Moussa and S. A. Ahmed, Room-Temperature CO Oxidation over Au-Pd Monometallic and Bimetallic Nanoparticle-Supported MgO, *ACS Appl. Nano Mater.*, 2023, **6**(6), 4243–4252.

74 J. Chen, Y. Su, Q. Meng, H. Qian, L. Shi, J. A. Darr, Z. Wu and X. Weng, Palladium Encapsulated by an Oxygen-Saturated TiO_2 Overlayer for Low-Temperature SO_2-Tolerant Catalysis during CO Oxidation, *Angew. Chem., Int. Ed.*, 2023, **62**(49), e202310191.

75 Y. Song, S. Svadlenak, T. Bathena, M. J. Hazlett, W. S. Epling, K. A. Goulas and L. C. Grabow, PdCu Alloy Catalyst for Inhibition-free, Low-temperature CO Oxidation, *Chemcatchem*, 2024, **16**(1), e202301024.

76 S. Shigenobu, H. Hojo and H. Einaga, Catalytic Oxidation of CO to CO_2 over CeO_2-Supported Pd–Cu Catalysts under Dilute O_2 Conditions, *Ind. Eng. Chem. Res.*, 2022, 15856–15865.

77 V. Mehar, A. Almithn, T. Egle, M.-H. Yu, C. R. O'Connor, M. Karatok, R. J. Madix, D. Hibbitts and J. F. Weaver, Oxophilicity Drives Oxygen Transfer at a Palladium–Silver Interface for Increased CO Oxidation Activity, *ACS Catal.*, 2020, **10**(23), 13878–13889.

78 H. Dong, M. Jung, Y. Zhang, S. Wang and S. Ding, Supported noble metal-based catalysts for thermal CO_2 hydrogenation to CO, *Mol. Catal.*, 2024, **560**, 114133.

79 M. Lotfi, A. A. Gomaa, J. Wei, X. Zhang, K. Qadir, A. Goldbach and W. Shen, Surface-dependent CO oxidation over Au/ZnO nanopyramids and nanorods, *Appl. Catal., A*, 2023, **666**, 119436.

80 R. E. Tankard, F. Romeggio, S. K. Akazawa, A. Krabbe, O. F. Sloth, N. M. Secher, S. Colding-Fagerholt, S. Helveg, R. Palmer, C. D. Damsgaard, J. Kibsgaard and I. Chorkendorff, Stable mass-selected AuTiOx nanoparticles for CO oxidation, *Phys. Chem. Chem. Phys.*, 2024, **26**(12), 9253–9263.

81 H. Liu, Z. Cao, S. Yang, Q. Ren, Z. Dong, W. Liu, Z.-A. Li, X. Chen and L. Luo, Geometric edge effect on the interface of Au/CeO_2 nanocatalysts for CO oxidation, *Nano Res.*, 2024, 4986–4993.

82 Q. Huang, D. Ren, J. Ding, C. Tang, H. Wang, W. Huang, X. Wen and Z. Zhang, Tailoring Au–CuO interfaces for enhanced activity in CO oxidation, *Appl. Surf. Sci.*, 2024, **651**, 159231.

83 A. Holm, B. Davies, S. B. Bibi, F. Moncada, J. Halldin-Stenlid, L. Paskevicius, V. Claman, A. Slabon, C.-W. Tai, E. C. dos-Santos and S. Koroidov, A Water-Promoted Mars-van Krevelen Reaction Dominates Low-Temperature CO Oxidation over Au–Fe_2O_3 but Not over Au–TiO_2, *ACS Catal.*, 2024, **14**(5), 3191–3197.

84 X. Wang, J. Zhao, H. Eliasson, R. Erni, A. Ziarati, S. McKeown Walker and T. Burgi, Very Low Temperature CO Oxidation over Atomically Precise Au_{25} Nanoclusters on MnO_2, *J. Am. Chem. Soc.*, 2023, **145**(50), 27273–27281.

85 Y. Adachi, J. Brndiar, M. Konopka, R. Turansky, Q. Zhu, H. F. Wen, Y. Sugawara, L. Kantorovich, I. Stich and Y. J. Li, Tip-activated single-atom catalysis: CO oxidation on Au adatom on oxidized rutile TiO_2 surface, *Sci. Adv.*, 2023, **9**(39), eadi4799.

86 L. A. Calzada, C. Louis, C. Wan Han, V. Ortalan and R. Zanella, Au-Ru/TiO_2 prepared by deposition-precipitation with urea: Relevant synthesis parameters to obtain bimetallic particles, *Appl. Catal., B*, 2020, **264**, 118503.

87 R. Manzorro, W. E. Celín, J. A. Pérez-Omil, J. J. Calvino and S. Trasobares, Improving the Activity and Stability of YSZ-Supported Gold Powder Catalyst by Means of Ultrathin, Coherent, Ceria Overlayers. Atomic Scale Structural Insights, *ACS Catal.*, 2019, **9**(6), 5157–5170.

88 C. Mochizuki, Y. Inomata, S. Yasumura, M. Lin, A. Taketoshi, T. Honma, N. Sakaguchi, M. Haruta, K.-i. Shimizu, T. Ishida and T. Murayama, Defective NiO as a Stabilizer for Au Single-Atom Catalysts, *ACS Catal.*, 2022, 6149–6158.

89 C. T. Campbell, N. Lopez and S. Vajda, Catalytic properties of model supported nanoparticles, *J. Chem. Phys.*, 2020, **152**(14), 140401.

90 M. Lin, C. Mochizuki, B. An, Y. Inomata, T. Ishida, M. Haruta and T. Murayama, Elucidation of Active Sites of Gold Nanoparticles on Acidic Ta_2O_5 Supports for CO Oxidation, *ACS Catal.*, 2020, **10**(16), 9328–9335.

91 T. Fujitani, I. Nakamura and A. Takahashi, H_2O Dissociation at the Perimeter Interface between Gold Nanoparticles and TiO_2 Is Crucial for Oxidation of CO, *ACS Catal.*, 2020, **10**(4), 2517–2521.

92 T.-M. Tran-Thuy, T.-L. Yu and S. D. Lin, How H_2O may influence ambient CO oxidation over Au/BN, *Appl. Catal., B*, 2022, **314**, 121492.

93 S. Zhao, F. Chen, S. Duan, B. Shao, T. Li, H. Tang, Q. Lin, J. Zhang, L. Li, J. Huang, N. Bion, W. Liu, H. Sun, A. Q. Wang, M. Haruta, B. Qiao, J. Li, J. Liu and T. Zhang, Remarkable active-site dependent H(2)O promoting effect in CO oxidation, *Nat. Commun.*, 2019, **10**(1), 3824.

94 X. Qin, M. Chen, X. Chen, J. Zhang, X. Wang, J. Fang and C. Zhang, Effects of the Metal–Support Interaction in Ru/CeO_2 Nanostructures on Active Oxygen Species for HCHO/CO Oxidation, *ACS Appl. Nano Mater.*, 2022, **5**(10), 15574–15582.

95 X. Du, Y. Lang, K. Cao, J. Yang, J. Cai, B. Shan and R. Chen, Bifunctionally faceted Pt/Ru nanoparticles for preferential oxidation of CO in H_2, *J. Catal.*, 2021, **396**, 148–156.
96 Z. Rafaj, J. Krutel and V. Nehasil, Oxygen Exchange between Catalyst and Active Support during CO Oxidation on Rh/CeO_2(111) and Rh/CeO_2(110): Isotope Labeled 18O Study, *J. Phys. Chem. C*, 2021, **125**(29), 15959–15966.
97 C. Lin, A. C. Foucher, Y. Ji, E. A. Stach and R. J. Gorte, Investigation of Rh–titanate ($ATiO_3$) interactions on high-surface-area perovskite thin films prepared by atomic layer deposition, *J. Mater. Chem. A*, 2020, **8**(33), 16973–16984.
98 M. J. Hulsey, B. Zhang, Z. Ma, H. Asakura, D. A. Do, W. Chen, T. Tanaka, P. Zhang, Z. Wu and N. Yan, In situ spectroscopy-guided engineering of rhodium single-atom catalysts for CO oxidation, *Nat. Commun.*, 2019, **10**(1), 1330.